

Studies on Gas Sensing Properties of $Mg_xCd_{1-x}Fe_2O_4$ System

Ashok B. Gadkari^{1*}, Tukaram J. Shinde², Appaso A. Wali³, Pramod N. Vasambekar⁴

¹Department of Physics and Electronics, GKG College, Kolhapur 416012, Maharashtra, India

²Department of Physics, KRP Kanya Mahavidyalaya, Isalmpur 415409, Maharashtra, India

³Department of Physics, Devchand College, Arjunnagar 591237, Maharashtra, India

⁴Department of Electronics, Shivaji University, Kolhapur 416004, Maharashtra, India

*Corresponding author: E-mail: ashokgadkari88@yahoo.com; Tel: (+91) 09423814704

DOI: 10.5185/amp.2019.6996

www.vbripress.com/amp

Abstract

Nanocrystallite ferrites samples with general formula $Mg_{1-x}Cd_xFe_2O_4$ ($x = 0, 0.2, 0.4, 0.6, 0.8, 1$) were prepared by oxalate co-precipitation method from high purity sulphates. The samples were characterized by XRD, SEM and FT-IR techniques. The phase identification of powder reveals single phase cubic spinel nature of materials. The gas sensing properties were studied for ethanol (C_2H_5OH), liquid petroleum gas (LPG) and chlorine (Cl_2). The $MgFe_2O_4$ is sensitive to LPG (~ 80%) followed by Cl_2 (~75%) and less to ethanol (~ 58%) at an operating temperature of 225°C. The sample with $x = 0.4$ has highest sensitivity at operating temperature 225°C for LPG (~ 78%). It shows good sensitivity at operating temperature at 198°C for Cl_2 (~75%) and ethanol (~ 65%). The $CdFe_2O_4$ sensor ($x=1$) exhibits very high sensitivity (85%) and good selectivity to ethanol than other tested gases such as LPG (~ 35%) and Cl_2 (~ 30%). The response and recovery time decreases with increase in Cd^{2+} content for LPG, Cl_2 and ethanol. The shorter response is observed to $CdFe_2O_4$ for LPG, Cl_2 and ethanol. Copyright © VBRI Press.

Keywords: Chemical synthesis, gas sensor, sensitivity, response time.

Introduction

The sensors are the devices which convert physical or chemical quantity into electrical signals convenient to use [1]. The increasing environmental pollution problems-detection of toxic gases, medicine, and agriculture insists the need of reliable and selective solid-state sensor for both air quality monitoring and control of automobile exhaust [2]. The gas sensors to detect reducing and oxidizing gases need to be developed. The wide range of sensor materials based on metal oxide semiconductors has been developed [3]. The sensitivity of such sensors increases with addition of catalytic metals and non metals.

Several researchers prepared ferrite gas sensors [2, 4, 5]. The Cu, Zn, Cd and Mg ferrite are prepared by Chen *et al.* [6] and tested for gases like CO, H₂, LPG and C₂H₂. They revealed that the sensitivity of ferrites depends on the type of ferrite, morphology and specific surface area. The zinc ferrite was used as hydrogen sensor by Mukherjee *et al.* [7]. They showed that the hydrogen adsorption and water adsorption control the response and recovery kinetics of gas sensing. Kadu *et al.* [8] studied Zn-Mn nanomaterials for reducing gases like LPG, CH₄, CO and C₂H₅OH. They seen high response to ethanol at an operating temperature of 300 °C. The gas sensing was investigated by Iftimie *et al.* [9] at operating temperature between 300 to 500 °C for ethyl alcohol, methane, liquefied petroleum gas,

formaldehyde and ammonia. They reported that the grain size, surface area and pores plays an important role for gas sensing purpose. Influence of Pd on gas sensing properties of magnesium ferrite was studied by Darshane *et al.* [10]. They found excellent sensitivity at 200 ppm for Pd doped magnesium ferrite. Liu *et al.* [11] reported magnesium ferrite and response was tested for CH₄, H₂S, LPG and C₂H₅OH. The Mg ferrite exhibited highest response to LPG. The semi conducting cadmium ferrite has been used as high performance ethanol sensor by Liu *et al.* [12]. The ferrite AFe_2O_4 with ($A = Zn, Cu, Co, Ni$) is studied by Gopal Reddy *et al.* [13] for detection of toxic gases and Cl_2 . The changes in pore size, porosity and specific area of the ferrite influences sensitivity. The large specific area results high sensitivity within certain limits [14, 15].

In this communication, we report investigations of sensing properties of Mg-Cd ferrites for gases such as LPG, Cl_2 and C₂H₅OH, synthesized by oxalate co-precipitation method.

Experimental

Synthesis and characterization

Mg-Cd ferrites with chemical formula $Mg_{1-x}Cd_xFe_2O_4$ ($x = 0, 0.2, 0.4, 0.6, 0.8$ and 1.0) were synthesized by the oxalate co-precipitation method [16]. High purity AR grade, $MgSO_4 \cdot 7H_2O$, $3CdSO_4 \cdot 8H_2O$ and $FeSO_4 \cdot 7H_2O$

were used as starting materials. The resulting precipitate was dried and presintered at 700 °C for 6 h in air. The presintered powder was milled to have fine powder and sintered at 1050 °C for 5h. The sintered powder was mixed with binder and pressed into the form of pellets having diameter 13 mm by applying pressure of 7 tones/cm². The pellets were finally sintered at 1050 °C for 5 h.

Philips PW-3710 X-ray powder diffractometer was used to study structure of ferrite. The morphological analyses of fractured pellets were taken on a scanning electron microscope (JEOL – JSM 6360 model, Japan). The FTIR of ferrites under investigation were recorded in the range of 350 cm⁻¹ to 800 cm⁻¹ on Perkin-Elmer FT-IR spectrum one spectrometer using KBr pellet technique.

Gas sensing

The gas sensitivity of all the ferrites under investigation were tested for C₂H₅OH, LPG, and Cl₂. The sensitivity (S) was calculated by using equation [15],

$$S(\%) = \frac{\Delta R}{R_a} \times 100 = \frac{|R_a - R_g|}{R_a} \times 100 \quad (1)$$

Results and discussion

Characterization

The XRD patterns, micrographs and IR absorption spectra of Mg-Cd ferrite samples under investigations are already reported [16]. The typical XRD pattern of MgFe₂O₄ is presented in Fig. 1. All the samples show single phase cubic spinel structure. The average crystallite size of the samples obtained from Debye Scherrer’s relationship is in the range 27.79 to 30.40 nm. Typical micrograph of CdFe₂O₄ is presented in Fig. 2. The average grain size in the samples is calculated by linear intercept method. It lies in the range of 0.58 μm to 1.2 μm. Typical IR absorption spectra of Mg_{0.6}Cd_{0.4}Fe₂O₄ is presented in Fig. 3. It shows two absorption bands in the frequency range of 350–800 cm⁻¹ which shows well formation of ferrites. The high and low frequency absorption bands (ν₁ and ν₂) are observed in frequency range of 555 to 576 cm⁻¹ and 431 to 472 cm⁻¹ respectively [16].

Gas sensing mechanism

Gas sensing mechanism of ferrite material is surface controlled type [9]. The metal ions on the surface of Mg-Cd ferrite sensors adsorb atmospheric oxygen by transferring electrons from conduction band to adsorbed oxygen atom, resulting in the formation of ionic species such as O⁻ or O⁻² (O⁻ is believed to be dominant at operating temperature 100-500 °C). With increasing operating temperature the state of oxygen adsorbed on the surface of Mg-Cd ferrite sensors under goes the following reaction [17],

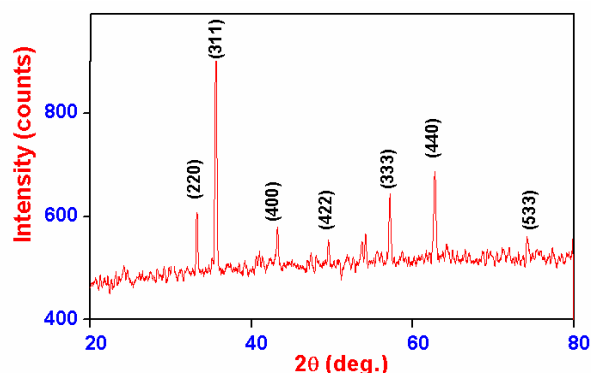


Fig. 1. Typical X-ray diffraction patterns of MgFe₂O₄ system (x = 0).

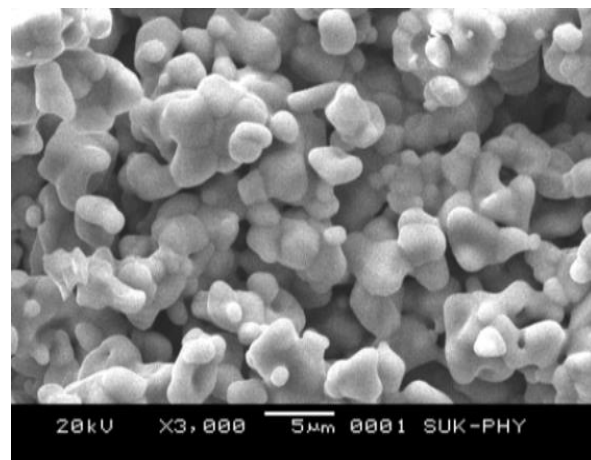


Fig. 2. SEM micrographs of CdFe₂O₄ system (x = 1).

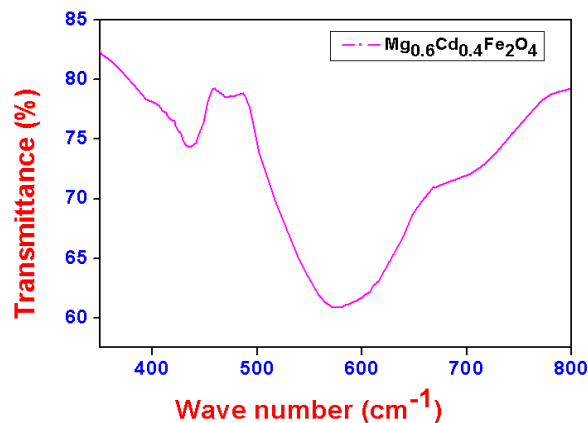
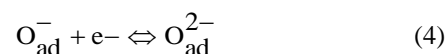
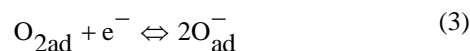
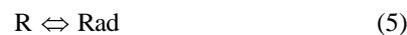


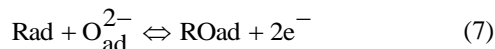
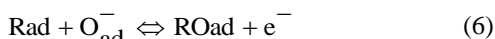
Fig. 3. Typical FT-IR spectra of Mg_{0.6}Cd_{0.4}Fe₂O₄ system (x = 0.4).



The oxygen species capture electrons from the conduction band of Mg-Cd ferrite sensors leading to decreased electron concentration resulting in increased resistance of the Mg-Cd ferrite sensors. When the reducing gases (R) are introduced, they are adsorbed on the surface of the Mg-Cd ferrite sensors as [5, 17],



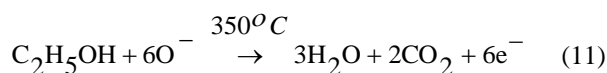
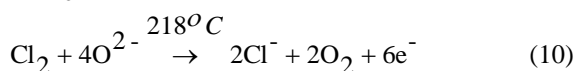
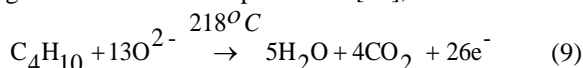
They react with O^- releasing the trapped electrons to the conduction band of the sensors subsequently lowering the resistance. The reaction between the adsorbed gas and the adsorbed oxygen is for example, O_{ad}^- and O_{ad}^{2-} will then be [17],



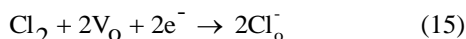
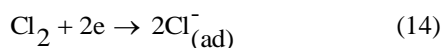
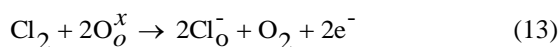
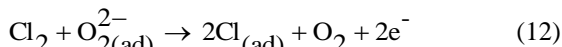
Finally desorption of the resulting product will take place as [17],



This explanation holds good for reducing gases under test. The possible reaction of these gases on the Mg-Cd sensor can be explained as [18],



There are four adsorption behavior of chlorine on the oxide surface [19-21].



Here subscript 'ad' and 'o' are the spaces adsorbed on the sensor surfaces and species occupying the lattice oxygen site respectively and V_o is the oxygen vacancy. These reaction shows n-type conduction mechanism of sensor. Thus, on the oxidation of single molecule of gas liberate plurality of electrons in the conduction band, resulting an increase in conductivity of the sensors.

In the reaction (12) and (13) chlorine substitute for adsorbed oxygen and lattice oxygen to form $Cl_{(ad)}^-$ and $Cl_{(o)}^-$ respectively, donating electron to Mg-Cd sensor. On the other hand in reaction (14) and (15) chlorine is adsorbed on the surface and occupies a oxygen vacancy to form $Cl_{(ad)}^-$ and $Cl_{(o)}^-$ respectively.

In this case, the electron are drawn from the oxide resulting in resistance therefore the oxygen adsorption-desorption mechanism is not employed to sense the Cl_2 gas and hence in the present case chlorine sensor surface is favorable mechanism [20, 21].

Sensitivity

Variation of sensitivity with operating temperature of cadmium substituted magnesium ferrites for LPG, Cl_2 and C_2H_5OH is presented in Fig. 4 (a-f). From this figure, it is observed that the sensitivity of all the samples under investigations, for each test gas, increases with increase in temperature, reaches

maximum corresponding to optimum operating temperature and decreases thereafter. The operating temperature is one of the important parameters that determine the sensitivity of the ceramic gas sensor. The response of the sensor (change in resistance) to presence of test gases depends on activation processes viz. speed of chemical reaction on surface of the grain and speed of the diffusion of the gas molecules to the surface. The activation energy of chemical reaction is higher. At low temperature response is restricted by speed of chemical reaction and at high temperature it is restricted by speed of diffusion of gas molecules. At intermediate temperature speed of two processes becomes equal. At this temperature the sensitivity is highest [14]. Thus in present investigation, for every gas there is specific temperature at which sensor sensitivity attains its peak value. The temperature corresponding to peak value is function of gas, chemical composition, additives and catalysts [22].

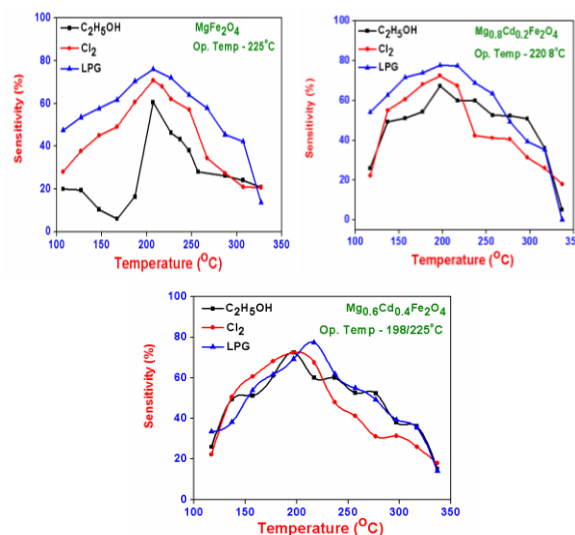


Fig. 4. Variation of sensitivity as a function of operating temperature of $Mg_{1-x}Cd_xFe_2O_4$ system.

a) $MgFe_2O_4$ b) $Mg_{0.8}Cd_{0.2}Fe_2O_4$ c) $Mg_{0.6}Cd_{0.4}Fe_2O_4$

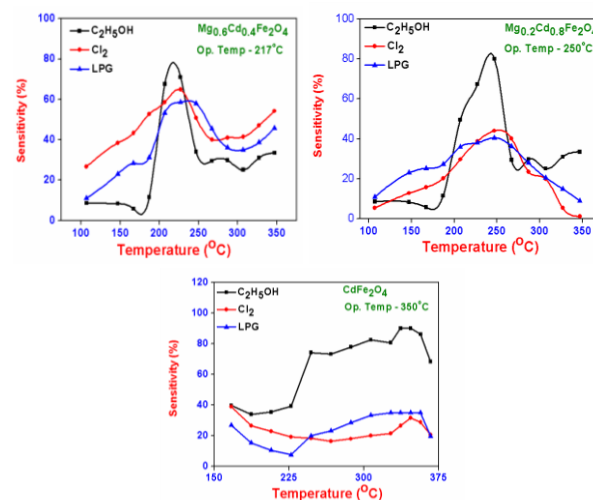


Fig. 4. Variation of sensitivity as a function of operating temperature of $Mg_{1-x}Cd_xFe_2O_4$ system.

d) $Mg_{0.4}Cd_{0.6}Fe_2O_4$ e) $Mg_{0.2}Cd_{0.8}Fe_2O_4$ f) $CdFe_2O_4$

The variation of gas sensitivity with Cd^{2+} content is presented in **Fig. 6**. From this figure, it is seen that, Mg ferrite sensor ($x = 0$) has highest sensitivity to LPG (~80%) followed by Cl_2 (~75%) and less to ethanol (~58%) at an operating temperature of 225 °C. The lower operating of Mg ferrite sensor is probably due to its large surface area and high surface activity which results strong interaction between LPG and chlorine and nanocrystallite Mg ferrite sensor. Liu *et al.* [11] also reported highest response of this sensor to LPG.

Iftimie *et al.* [9] reported high sensitivity to LPG at operating temperature of 450 °C for Mg-Mn ferrites. The operating temperature of Mg ferrite sensor under investigation is lower than that reported [6, 10]. Rezlescu *et al.* [23] reported Mg ferrite with addition of Sn and Mo ions. They reported higher sensitivity for Sn doped Mg ferrite than Mo substitution compared to pure magnesium ferrite. They attributed the faster response of Sn substituted Mg ferrite to From **Fig. 5** and **Fig. 4 (c)** it can be noticed that $\text{Mg}_{0.6}\text{Cd}_{0.4}\text{Fe}_2\text{O}_4$ has good sensitivity to LPG (~78%) at an operating temperature of 225 °C, Cl_2 (~75%) at 198 °C and ethanol (~65%) at the same temperature. This slight reduction in operating temperature from 225-198 °C for Cl_2 and ethanol can be attributed to the changed composition of the sensor. Similar results are reported by Satanarayana *et al.* [15] for Ni-Co ferrites.

From **Fig. 5** and **Fig. 4(f)** it can be noticed that at operating temperature of 350 °C, Cd ferrite sensor ($x = 1$) exhibits highest sensitivity (85%) to ethanol than that for LPG (~35%) and Cl_2 (~30%). The requirement of higher operating temperature is probably because of smaller specific area and lower surface activity of this sensor, resulting in weaker interaction between test gases and sensor surface [6, 12]. Chen *et al.* [6] also reported similar results for Zn ferrite. For mixed ferrite sensors the sensitivity depends on operating temperature and composition. **Fig. 5** further shows that the increment of Cd^{2+} in Mg ferrite sensors has increased the selectively to ethanol. More ever the increase of Cd^{2+} content improved the selectively to ethanol while by decreasing the sensitivity to other reducing gases LPG and Cl_2 . Jiao *et al.* [24] also reported that, sensitivity and selectivity of the sensor can be controlled by conditions under which reactions takes place at the surface. They also reported relationship between the flow rate and crystal size. The crystallite size decreases with increases in gas flow rate.

Response-Recovery time

The time taken by sensor element to achieve highest maximum sensitivity and time to come back at original value when test gas is removed at an operating temperature are the response and recovery time [13]. The typical response and recovery characteristics of MgFe_2O_4 , $\text{Mg}_{0.6}\text{Cd}_{0.4}\text{Fe}_2\text{O}_4$ and CdFe_2O_4 are presented in **Fig. 6 (a, b, c)**. It is seen that the response time of Mg ferrite at operating temperature of 225°C to LPG, Cl_2 and ethanol is same (300s). From **Fig. 6 (b)** it can be seen that the response time of $\text{Mg}_{0.6}\text{Cd}_{0.4}\text{Fe}_2\text{O}_4$

sensor, at operating temperature of 198°C to LPG, Cl_2 is 250s, and 300s for ethanol respectively i.e. response and recovery time for this sensor have been reduced compared to that for Mg ferrite sensor. The response time of Cd ferrite sensor, is 200s for LPG, Cl_2 and 250s for ethanol. This response of Cd ferrite sensor is lower as compared to all the other samples. This may be due to highest porosity of cadmium ferrite [23, 24]. The poor recovery time is observed for all the samples due to bulk nature of sensing material. When Mg-Cd sensor is exposed to test gas it goes deep er inside the sensor and comes out slowly which gives longer recovery time.

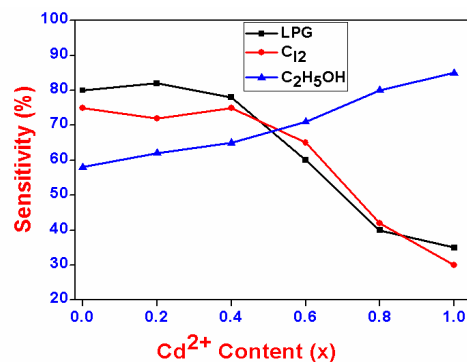


Fig. 5. Variation of gas sensitivity as a function of Cd^{2+} content.

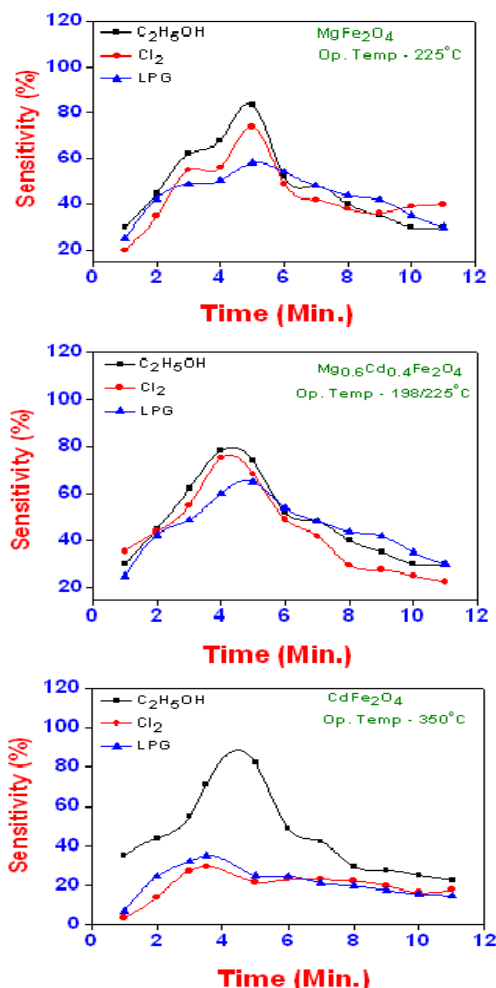


Fig. 6. Response and recovery characteristics of $\text{Mg}_{1-x}\text{Cd}_x\text{Fe}_2\text{O}_4$ system (a) MgFe_2O_4 (b) $\text{Mg}_{0.6}\text{Cd}_{0.4}\text{Fe}_2\text{O}_4$ (c) CdFe_2O_4

Conclusion

Mg-Cd ferrites under investigation have single phase cubic spinel structure. Their average crystallite size lies in the range of 27.79 to 30.40 nm. Mg ferrite sensor exhibits high sensitivity to LPG and Cl_2 at 225 °C as compared to that of other samples which is attributed to smaller grain size. $\text{Mg}_{0.6}\text{Cd}_{0.4}\text{Fe}_2\text{O}_4$ showed good response and selectivity to LPG, Cl_2 and $\text{C}_2\text{H}_5\text{OH}$. Cd ferrite sensor exhibited high sensitivity and good selectivity to ethanol than other tested gases. The shorter response and recovery time is observed for Cd ferrite sensor compared to Mg ferrite and $\text{Mg}_{0.6}\text{Cd}_{0.4}\text{Fe}_2\text{O}_4$ sensor. The response and recovery times depend on type of gas and composition. The resulting sensitivity and response /recovery time indicates that particularly Mg, $\text{Mg}_{0.6}\text{Cd}_{0.4}\text{Fe}_2\text{O}_4$ and Cd ferrites should be good materials for the fabrication of LPG and $\text{C}_2\text{H}_5\text{OH}$ sensors respectively. The gas sensitivity depends largely on microstructure, working temperature, type of substitution and test gas.

References

1. Gopal, W.; Hesse, J.; Zemel, J. N.; Fundamental and General Aspects, Sensors; Weinheim VCH, Verlagsgesellschaft mbH, **1989**, 1, 304.
2. Dos Santos-Alves, J. S. G.; Patier, R. F.; *Sens. Actuators B*, **1999**, 59, 69.
3. Tsang, S. C.; Bulpitt, C.; *Sens. Actuators B*, **1998**, 52, 226.
4. Gadkari, A. B.; Shinde, T. J.; Vasambekar, P. N.; *IEEE Sensors J.*, **2011**, 11, 849.
5. Tianshu, Z.; Hing, P.; Jiancheng, Z.; Lingbing, K.; *Mater. Chem. Phys.*, **1999**, 61, 192.
6. Chen, N. S.; Yang, X. J.; Liu, E. S.; Huang, J. L.; *Sens. Actuators B*, **2000**, 66, 178.
7. Mukherjee, K.; Majumdar, S. B.; *J. Appl. Phys.*, **2009**, 106, 064912.
8. Kadu, A. V.; Jagtap, S. V.; and Chaudhari, Q. N.; *Current Appl. Phys.*, **2009**, 9, 1246.
9. Iftimie, N.; Rezlescu, E.; Popa, P. D.; Rezlescu, N.; *J. of Optoelectro. Adv. Mater.*, **2006**, 8, 1001.
10. Darshane, S.; Mulla, I. S.; *Mater. Chem. Phys.*, **2010**, 119, 319.
11. Liu, Y.; Liu, Z. M.; Yang, Y.; Yang, H. F.; Shen, G. L.; Yu, R. Q.; *Sens. Actuators B*, **2005**, 107, 600.
12. Liu, X. Q.; Xu, Z.; Liu, Y.; Shen, Y.; *Sens. Actuators B*, **1998**, 52, 270.
13. Gopal Reddy, C. V.; Manorma, S. V.; Rao, V. J.; *J. Mater. Sci. Letts.*, **2000**, 19, 775.
14. Nenov, T. G.; Yordanov, S. P.; Ceramic Sensors, Technology and Application; Lancaster, Technomic Publishing Company, USA; **1996**, 20-42, 134.
15. Satyanarayana, L.; Reddy, K. M.; Manorama, S.V.; *Mater. Chem. Phys.*, **2003**, 82, 21.
16. Gadkari, A. B.; Shinde, T. J.; Vasambekar, P. N.; *J. of Material Science: Material in Electronics*, **2010**, 21, 1, 96.
17. Tao, S.; Gao, F.; Liu, X., and Sorensen, O. T.; *Mater. Sci. Engin. B*, **2000**, 77, 172.
18. Bangale, S.V.; Patil D.R.; Bamane, S.R.; *Sensors and Transducers Journal*, **2011**, 134, 107.
19. Dawson D. H.; Williams, D. E.; *J. Mater. Chem.*, **1996**, 6, 406.
20. Chu, X. F.; *Mater. Res. Bull.*, **2006**, 51, 631.
21. Kamble, R. B.; Mathe, V. L.; *Sens. Actuators B: Chem.*, **2008**, 131, 205.
22. Yamzoe N.; Miura, N.; IEEE Transaction of Components Packing, Manufacturing Technology, **1996**, 18, 252.
23. Rezlescu, N.; Doroftei, C.; Rezlescu, E.; Popa, P. D.; *Phys. Stat. Solidi A*, **2006**, 203, 306.
24. Zheng, J.; Minghoog, W.; Jianzhong G.; Zheng, Q.; *IEEE Sens. J.*, **2003**, 3, 435.
25. Liu, X. Q.; Xu, Z. L.; Shen, Y. S.; J. Yuman Uni., **1997**, 19, 147.